Coordination Chemistry Reviews, 49 (1983) 76—116
Elsevier Scientific Publishing Company, Amsterdam — Printed in The Netherlands

Chapter 2

ELEMENTS OF GROUP 2

Peter Hubberstey

0010-8545/83/$12.30

2.1 INTRODUCTION

The pattern adopted previously[1] for reporting the chemistry of these elements has been retained for the present review. Thus, the abstracted data are considered in sections which reflect topics currently of interest and importance. Some of the topics (e.g. molten salts, acyclic and macrocyclic polyether complexes) are common to Group I and Group II elements; for these, the published data are considered in the relevant section in Chapter 1. The topics unique to the Group II elements are discussed in this Chapter.

Annual surveys, covering 1978[2] and 1979[3], of the organometallic chemistry of magnesium have been published during the period of this review; preparative routes to organomagnesium compounds, their spectroscopic and structural properties and their reaction chemistry are discussed in detail.

Ultrapure samples of Ca, Sr and Ba have been prepared[4] by metallothermic reduction of their high purity oxides with high purity aluminium in ultrahigh vacuum. Unfortunately, the vapour pressure of aluminium at the reduction temperature results in contamination of the alkaline earth metal condensates. Subsequent ultrahigh vacuum distillation, however, markedly reduces the aluminium impurity content. The metals were characterised by trace analytical techniques, the major impurities being the other alkaline earth metals and aluminium (Table 1)

Table 1. Non-metallic and metallic impurities in high purity alkaline earth metals.[4]

Impurity*	Alkaline earth metal					
	Ca		Sr		Ba	
	wppm	appm	wppm	appm	wppm	appm
H	17	680	42	3700	15	2100
N	5	14	5	31	5	49
Mg	< 1	< 1	< 1	< 1	< 1	< 1
Ca	-	-	46	100	< 1	< 1
Sr	16	7	-	-	< 1	< 1
Ba	1	< 1	< 1	< 1	-	-
Al	22	33	13	42	< 2	< 10

* oxygen impurity was not determined.

The capillary-tube isotachophoresis technique has been developed[5] for the simultaneous determination of Mg^{2+}, Ca^{2+}, Sr^{2+} and Ba^{2+} at electrolyte pH ≥5.5; the relative standard deviations were 1.7 - 2.2% for the determination of 15-25 nmol of the cations at electrolyte pH = 5.70.

Calcium isotope separation has been studied in detail by Heumann et al.[6,7] $^{40}Ca/^{48}Ca$ and $^{40}Ca/^{44}Ca$ separation has been assessed in the H_2O-$CHCl_3$ liquid-liquid extraction system both in the presence and absence of C221 and C222 as complexing agents.[6] In the absence of a complexing agent, ^{40}Ca is enriched in the $CHCl_3$ phase (α=1.011 for $^{40}Ca/^{48}Ca$; α=1.004 for $^{40}Ca/^{44}Ca$). Although C221 has only marginal effect on the separation (α=1.011 for $^{40}Ca/^{48}Ca$; α=1.006 for $^{40}Ca/^{44}Ca$), with C222 the separation is markedly higher (α=1.015 for $^{40}Ca/^{48}Ca$; α=1.008 for $^{40}Ca/^{44}Ca$). $^{40}Ca/^{48}Ca$ separation has also been investigated in the strongly acidic cation exchanger-aqueous $BaCl_2$ solution resin-liquid extraction system.[7] ^{48}Ca is enriched in the liquid phase, whereas ^{40}Ca is enriched in the resin phase; the separation effect increases with both decreasing $BaCl_2$ concentration and temperature.

2.2 METALS AND INTERMETALLIC COMPOUNDS

In contrast to the 1980 review[1], far fewer papers have been abstracted on these topics. Consequently the format adopted for this section is similar to that for the 1979 review[8] where the data were considered en bloc rather than in a series of subsections as in the 1980 review.[1]

Charge transfer calculations[9] in Mg-Sn solutions indicate that the elctron charge transfers from tin to magnesium; at the $Mg_{0.5}Sn_{0.5}$ stoichiometry it is ca. 0.85 electrons per atom.

Phase relationships have been elucidated in the Ca-Pt ($0.00 \leq x_{Pt} \leq 0.50$),[10] Sr-Pt ($0.00 \leq x_{Pt} \leq 0.50$),[10] Sr-Sn ($0.00 \leq x_{Sn} \leq 0.67$;[11] $0.65 \leq x_{Sn} \leq 1.00$[12]) and Sr-Pb ($0.00 \leq x_{Pb} \leq 1.00$)[13] binary systems. The corresponding phase diagrams are shown in Figure 1; although those for the Ca-Pt,[10] Sr-Pt[10] and Sr-Pb[13] systems are as published, that for the Sr-Sn system is a composite of those in the two original publications.[11,12] Available structural data for the various intermetallic compounds formed in the four systems are summarised in Table 2.

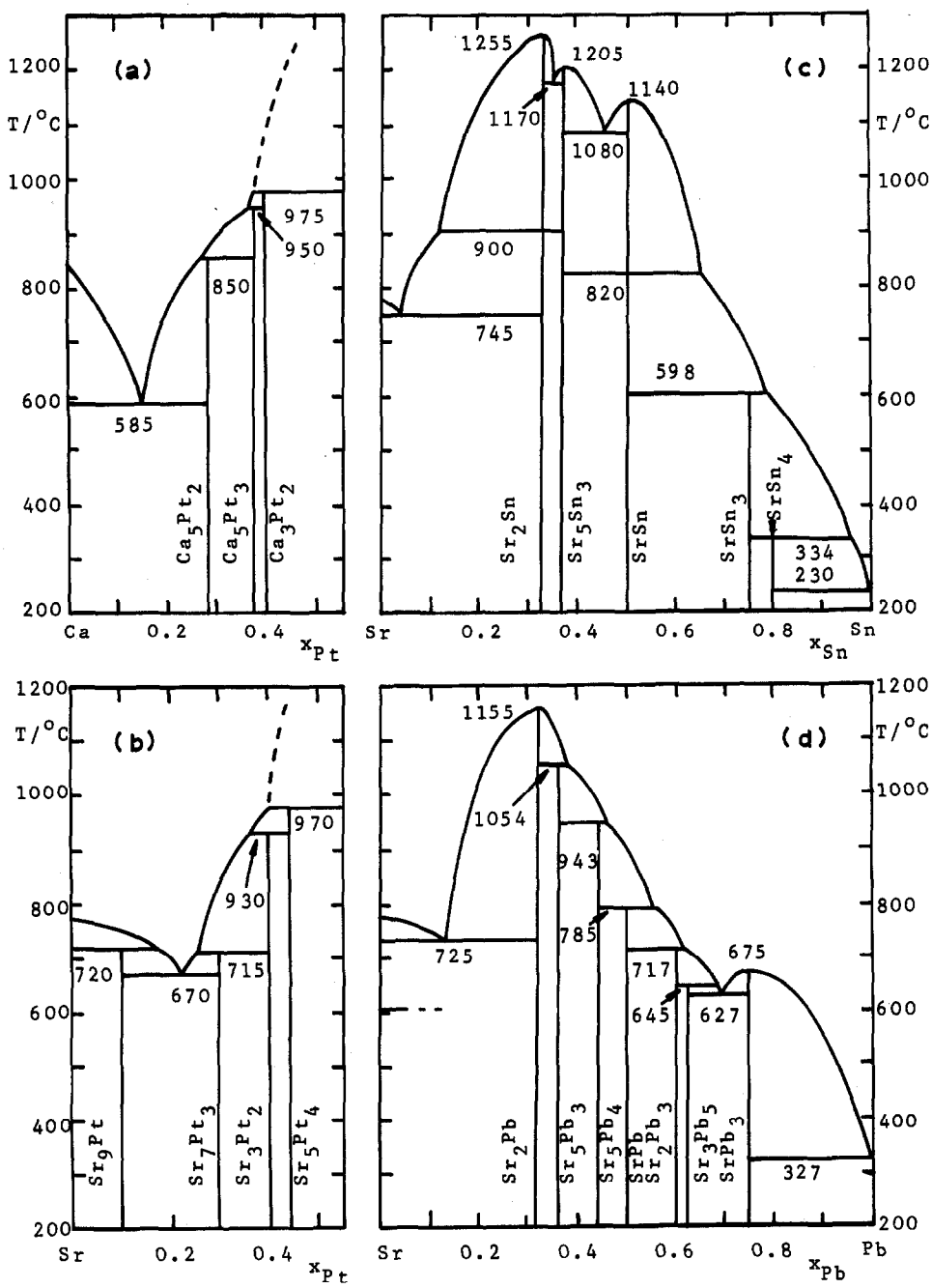

Figure 1. Phase diagrams of the (a) Ca-Pt, (b) Sr-Pt, (c) Sr-Sn and (d) Sr-Pb binary systems.

Table 2. Crystallographic parameters for the intermetallic compounds formed in the Ca-Pt, Sr-Pt, Sr-Sn and Sr-Pb binary systems.

Intermetallic compound	Symmetry	Space Group	a/pm	b/pm	c/pm	β/°	Ref.
Ca_5Pt_2	monoclinic	C2/c	1615.4	662.7	766.2	97.47	10
Ca_5Pt_3	tetragonal	I4/mcm	1156.3		575.3		10
Ca_3Pt_2	rhombohedral	$R\bar{3}$	878.6		1678.6		10
Sr_9Pt	cubic		609.1				10
Sr_7Pt_3	orthorhombic	Pnma	793.7	2433.3	710.9		10
Sr_3Pt_2	rhombohedral	$R\bar{3}$	933.7		1776.2		10
Sr_5Pt_4	orthorhombic	Pnma	787.9	1560.6	814.7		10
Sr_2Sn	orthorhombic	Pnma	840.2	537.8	1007.8		11
Sr_5Sn_3	tetragonal	(Cr_5B_3)	856.5		1626.1		11
SrSn	orthorhombic	Cmcm	503.3	1200	449.3		11
$SrSn_3$	rhombohedral	$R\bar{3}m$	1200		3294		11
Sr_2Pb	orthorhombic	(anti-$PbCl_2$)	844.5	539.1	1013.9		13
Sr_5Pb_3	tetragonal	(Cr_5B_3)	867		1594		13
Sr_5Pb_4	orthorhombic	(Gd_5Si_4)	848	1727	901		13
SrPb	orthorhombic	(CrB)	501.8	1223	464.8		13
Sr_2Pb_3	tetragonal	P4bm	838		490		13
Sr_3Pb_5	tetragonal	P4bm	1618		490		13
$SrPb_3$	tetragonal	(Ti_3Cu)	496.5		503.5		13

Structural studies have also been effected for Ca_3Zn,[14] CaZn,[14] α-CaCu,[15] β-CaCu,[15] SrAg and BaAg;[15] unit cell parameters are collected in Table 3. The structures of the equimolar intermetallic compounds are very similar; they are all based on the same trigonal prismatic coordination around the noble metals and differ only in the arrangement and sequence of the prisms along the a axis.[15]

Pearson has undertaken a dimensional analysis of Laves phases with the $MgCu_2$[16] and $MgZn_2$[17] structures. The unit cell dimensions of the two structures are shown to vary regularly with the CN12 diameters of the component atoms; equations are derived for the calculation of unit cell parameters from ionic diameters.[16] Pearson has also shown[18] that the unit cell parameters of triads of intermetallic phases, M_xN_y, where M is Ca, Sr and Ba (or Sc, Y and La), follow more closely a linear function of the M component atomic numbers than of their CN12 diameters. This is shown to be a triviality resulting from the fact that the atomic arrays which control the cell dimensions of phases containing barium (or the rare earths) are different from those that control the cell dimensions of phases containing calcium and strontium (or scandium and yttrium).[18]

The magnetic properties of Mg_5Eu have been determined ($3.7 \leqslant T/K \leqslant 295$).[19] Above 20K it exhibits Curie-Weiss behaviour with $\mu=7.9\mu_B$ and $\theta=+7.5K$; at low temperatures, magnetic ordering of the antiferromagnetic type occurs.

Standard thermodynamic parameters for the formation of various calcium-containing intermetallic compounds have also been evaluated from hydrogen titration[20] and potentiometric[21] measurements; the data are collected in Table 4.

Several authors[22-26] have investigated the reaction of hydrogen with intermetallic compounds containing alkaline earth metals. Relationships between intermetallic compound structure and hydride formation have been considered[22] for hexagonal $AB_5(D_{2d})$, cubic $AB_2(Cl5)$, hexagonal $AB_2(Cl4)$ and orthorhombic $AB(B_\gamma)$ compounds. The structural analysis involves the number, size, position and symmetry properties of tetrahedral interstitial holes; holes and clusters of holes are considered in terms of their suitability for hydrogen occupancy in the formation of intermetallic compound hydrides.

In situ X-ray diffraction studies of the product of the reaction

Table 3. Crystallographic parameters for a number of intermetallic compounds.

Intermetallic compound	Symmetry	Space Group	a/pm	b/pm	c/pm	β/°	Ref.
Ca_3Zn	orthorhombic	Cmcm	415.0	1325.8	1018.6		14
CaZn	orthorhombic	Cmcm	420.2	1161	444.2		14
α-CaCu	orthorhombic	Pnma	3880	427.1	589.4		15
β-CaCu	monoclinic	$P2_1/m$	1947	427.1	588.0	94.3	15
SrAg	orthorhombic	Pnma	1655.8	478.8	638.5		15
BaAg	orthorhombic	Pnma	865.7	498.2	665.1		15

Table 4. Standard thermodynamic parameters for the formation of several intermetallic compounds.

Intermetallic compound	$-\Delta H_f^o(X,c,298K)$ kJ mol^{-1}	$-\Delta S_f^o(X,c,298K)$ J K^{-1} mol^{-1}	$-\Delta G_f^o(X,c,298K)$ kJ mol^{-1}	$-\Delta G_f^o(X,c,800K)$ kJ mol^{-1}	Reference
$CaAl_2$	93.84	17.01	88.77	80.23	20
$CaAl_4$	100.90	21.45	94.51	83.74	20
CaAg				50.0	21
$CaAg_2$				67.5	21
Ca_2Ag_7				170.1	21
Ca_2Ag_9				172.7	21

of hydrogen with Mg_2Ni[23] and with $CaNi_5$[24] have been effected. The hydride phase formed by Mg_2Ni is tetragonal (a=1139.4, c=749.9 pm); it undergoes a polymorphic phase transition at 503K to form an orthorhombic structure (a=1139.4, b=1119.6, c=916.5pm). The hydride phase formed by $CaNi_5$ is orthorhombic (a=525.0, b=919.4, c=804.2 pm). The compositions of the products conform to the stoichiometries, Mg_2NiH_4 and $CaNi_5H_5$, respectively.[23,24]

Alloying of small amounts of nickel or indium with Mg-Al intermetallic compounds has been shown[25] to cause a significant increase in the hydrogenation rates of these compounds.

The material formed when Mg_3Sn was treated with anthracene in thf at room temperature for several days readily absorbs hydrogen at room temperature and catalyses the hydrogenation of ethene.[26] It is concluded that complexing Mg_3Sn with anthracene gives rise to sites available for hydrogen activation as in the alkali metal-anthracene systems.

2.3 SIMPLE COMPOUNDS OF THE ALKALINE EARTH METALS

The change of emphasis adopted for the 1980 review, in which separate subsections were devoted to binary, ternary and quaternary derivatives of the alkaline earth metals, has been retained. Once again, the majority of papers abstracted describe the chemistry of novel quaternary oxides based on the perovskite structure.

2.3.1 Binary Derivatives

Although many papers have been published on the catalytic properties of the alkaline earth metal oxides, they are not considered here, since their content is of only peripheral interest to the inorganic chemist.

The cohesive energies of the alkaline earth metal chalcogenides MX (M = Mg-Ba; X = O-Te) with the NaCl structure have been evaluated[27] within the framework of the Born model; the resulting values are in close agreement with available experimental thermodynamic data. The structures of Ba_5Sb_4,[28] $BaSe_2$,[29] $BaSe_3$[29] and a high pressure polymorph of BaI_2[30] have been elucidated by X-ray diffraction methods; pertinent unit cell parameters are collected in Table 5. The crystal and molecular structures of $MgI_8.6H_2O$[31] and $CaI_{10}.7H_2O$[32] have also been determined. Whereas the structure of the former polyiodide consists of $[Mg(H_2O)_6]^{2+}$

and I_8^{2-} ions, that of the latter polyiodide consists of $[Ca(H_2O)_7]^{2+}$ and I_5^- ions. The Mg^{2+} coordination polyhedron is a slightly distorted octahedron, r(Mg...O) = 203.8-206.8; that of the Ca^{2+} ion is a distorted monocapped trigonal prism, r(Ca...O) = 233.5-244.8 pm.

Table 5. Crystallographic data for several barium salts.

Compound	Symmetry	Space Group	a/pm	b/pm	c/pm	β/°	Ref.
Ba_5Sb_4	orthorhombic	Pnma	901.2	1782.3	904.1		28
$BaSe_2$	monoclinic	C2/c	982.0	492.9	933.5	118.48	29
$BaSe_3$	tetragonal	$P\bar{4}2_1m$	728.0		425.0		29
BaI_2	hexagonal	$P\bar{6}2m$	914.7		517.3		30

Mechanistic studies[33] of the formation of alkaline earth metal fluorides MF_2 (M = Ca-Ba) by reaction of NH_4F or $NH_4.HF_2$ with MO (M = Ca-Ba) have been undertaken. Both materials can act as fluorinating agents but at high temperature (>453K) the reaction involving NH_4F is complicated by its decomposition to $NH_4.HF_2$ and NH_3.

The photolytically induced decomposition of $Ba(N_3)_2$ ($173 \leqslant T/K \leqslant 373$),[34] $Sr(N_3)_2$ ($183 \leqslant T/K \leqslant 363$),[34] and mixtures thereof ($408 \leqslant T/K \leqslant 463$)[35] have been studied in detail; kinetic analyses, the determination of activation energies and studies of the effect of light intensity have been undertaken.

A scheme for the hydrolytic precipitation equilibria of Mg^{2+} in aqueous $NaNO_3$ (1.0 mol dm^{-3}) at 298K has been presented.[36] When the solution is saturated with $Mg(OH)_2$, species such as Mg^{2+}, $[Mg_2(OH)_2]^{2+}$, $[Mg_3(OH)_4]^{2+}$ and $[Mg(OH)_2]$ are thought to be present in solution; their stability constants and solubility products were determined. Transpiration studies[37] of the calcium oxide-water vapour system ($1678 \leqslant T/K \leqslant 2016$; $1.2 \times 10^{-2} \leqslant P_{H_2O}/atm \leqslant 4.7 \times 10^{-1}$) have shown the predominant reaction to be that described by equation (1); derived thermodynamic data for this reaction are:

$$CaO(s) + H_2O(g) \rightleftharpoons Ca(OH)_2(g) \qquad \ldots(1)$$

$\Delta H_r^o(298K) = 261.9 \pm 3.3$ kJ.mol^{-1}, $\Delta S_r^o(298K) = 58.2 \pm 2.1$ JK^{-1}mol^{-1}, $\Delta G_r^o(298K) = 244.6 \pm 3.3$ kJ.mol^{-1}.[37] ^{2}H double resonance n.m.r. studies[38] of some anhydrous and hydrated alkaline earth metal (Sr,Ba) hydroxides have been undertaken; the ^{2}H quadrupole coupling constants of the OH^- ion are correlated with the stretching force constants.

2.3.2 Ternary Pnictides

Schafer et al[39,40] have reported the preparation and characterisation of a number of ternary pnictides containing an alkaline earth metal and a transition metal; typical unit cell parameters for compounds of stoichiometry $A_9B_4X_9$ and ABX_2 (A = Ca, Sr, Ba; B = Mn, Zn, Cd; X = Sb, Bi) are collected in Table 6.

2.3.3 Ternary Oxides and Chalcogenides

Ternary oxides in the $BaO-Fe_2O_3$ system have been characterised by X-ray diffraction and chemical analytical methods.[41] Five of the six oxides ($Ba_5Fe_2O_8$, $Ba_3Fe_2O_6$, $Ba_2Fe_2O_5$, $BaFe_2O_4$, $BaFe_{12}O_{19}$) are readily synthesised by heating appropriate stoichiometric mixtures of $BaCO_3$ and Fe_2O_3. The sixth oxide ($Ba_2Fe_6O_{11}$) could not be synthesised directly, presumably owing to the similarity of its stability with that of the mixture $BaFe_{12}O_{19} + 9BaFe_2O_4$; it was eventually prepared from $B_2O_3-Fe_2O_3-BaO$ ternary melts.[41] The process occuring when $CaCO_3$ is heated with FeO[42] and FeV_2O_4[43] in both inert and oxidising atmospheres has been investigated. In an inert atmosphere, interaction takes place as a direct redox process between the reagents. In an oxidising atmosphere, Fe^{2+} and V^{2+} are initially oxidised (to Fe^{3+} and V^{5+}, respectively) and then there is successive interaction of the oxidation products with $CaCO_3$.

The magnetic properties of the ternary oxides conforming to the K_2NiF_4 and α-$NaFeO_2$ structural types has been reviewed;[44] the relationship between structure and magnetic behaviour is stressed.

Structural parameters for $SrV_{10}O_{15}$,[45] $SrNb_2O_6$,[46] Ba_2MnO_3,[47] and $Be_4Pr_9O_{20}$[48] have been obtained from X-ray diffraction data; they are collected in Table 6. Isomorphism of alkaline earth metal orthovanadates $M_3(VO_4)_2$ (M = Ca-Ba) has been discussed in detail.[49] Although $Sr_3(VO_4)_2$ and $Ba_3(VO_4)_2$ are mutually soluble in the solid state, $Ca_3(VO_4)_2$ exhibits limited solid solubility with both $Sr_3(VO_4)_2$ and $Ba_3(VO_4)_2$.

Non-stoichiometry of polycrystalline $SrTiO_3$ has been studied using a resistivity technique.[50] Reduction processes, excess TiO_2 and acceptor impurities all contribute to oxygen vacancy content. The effect of donor impurities is dependent on the presence of excess TiO_2.[50]

The enthalpy of formation of the bronze, α-MgV_3O_8 ($\Delta H_f^o(\alpha\text{-}MgV_3O_8,c,298K) = -2917.53\pm0.45$ kJ mol^{-1}) has been determined[51] from an emf study of the thermodynamic characteristics of the oxidation of the bronze, α-$Mg_{1+x}(V_3O_8)_2$. The electrical properties of $BaLnO_4$ (Ln = Ce-Lu,Y,In)[52] and the luminescence of Mn(IV) in $CaZrO_3$[53] have also been investigated. Thermal treatment of $BaLnO_4$ in a reducing atmosphere (H_2) leads to a marked decrease in resistance ($x10^{-2}$-10^{-3}); thermal treatment in a vacuum, however, leads to a much lower decrease in resistance ($x10^{-1}$).

Thermal decomposition of $SrOsO_3$ in air can be represented by equation (2).[54] The reaction is complex, however, involving a

$$2SrOsO_3 \rightarrow 2SrO + Os + OsO_4 \quad \ldots(2)$$

phase transition in $SrOsO_3$ (orthorhombic to cubic at 1033±10K), formation of $Sr_2Os_2O_{6.4\pm0.2}$ (in the range 1243-1293K) and subsequent decomposition of $Sr_2Os_2O_{6.4\pm0.2}$ to SrO, Os and OsO_4 (at 1338±6K).

The synthesis and structural characterisation of three ternary sulphides, $BaVS_3$,[55] Ba_2HgS_3[56] and $BaHgS_2$[57] have been reported; unit cell parameters for these three materials are included in Table 6. $BaVS_3$, which is hexagonal at room temperature (Table 6) undergoes a crystallographic phase transition at ca. 250K.[55] The crystal symmetry becomes orthorhombic and twin formation (by pseudo-merohedry) is observed at the transition. Precession photographs of twinned crystals have been indexed in an orthorhombic cell with $a_o \sim a_h$, $b_o \sim \sqrt{3}a_h$ and $c_o \sim c_h$; the possible space groups are $Cmc2_1$ or $C222_1$.

2.3.4 Ternary Halides

The formation of ternary compounds containing MgF_2 and MF_n has been reviewed;[58] a correlation is shown to exist between ternary fluoride formation and the physicochemical properties (generalised moment, electronegativity) of the second component, M.

Solid solutions, $(Ca,Ln)_3F_7$ (Ln = Y, La-Lu), have been formed by annealing 2:1 CaF_2:LnF_3 molar mixtures at 1223-1273K.[59] X-ray

Table 6. Crystallographic parameters for various ternary pnictides, oxides, sulphides and halides.

Compound	Symmetry	Space Group	a/pm	b/pm	c/pm	β/°	Ref.
$Ca_9Zn_4Sb_9$	orthorhombic	Pbam	2192	1250	454		39
$CaMnSb_2$	orthorhombic	Pnma	2211	431.2	434.4		40
$SrMnSb_2$	orthorhombic	Pnma	2319	442	446		40
$BaMSb_2$ (M=Zn,Cd)*	tetragonal	I4/mmm	458.4		2305		40
$Ca_9Cd_4Bi_9$	orthorhombic	Pbam	2258	1278	474		39
$Sr_9Cd_4Bi_9$	orthorhombic	Pbam	2347	1327	489		39
$SrCdBi_2$	tetragonal	I4/mmm	463.5		2288		40
$BaMBi_2$ (M=Zn,Cd)*	tetragonal	I4/mmm	484.6		2198		40
$SrV_{10}O_{15}$	orthorhombic	Ccmb	991.5	1157.4	932.4		45
$SrNb_2O_6$	monoclinic	$P2_1/c$	772.2	559.2	1098.9	90.36	46
Ba_2MnO_3	monoclinic	Cc	584	1157	1270	93.7	47
$Be_4Pr_9O_{20}$	orthorhombic	$Pna2_1$	954.1	655.7	722.7		48
$BaVS_3$	hexagonal	$P6_3/mmc$	672.8		562.6		55
Ba_2HgS_3	orthorhombic	Pnma	893	435	1725		56
$BaHgS_2$	orthorhombic	$Pmc2_1$	421	1438	733		57

Table 6 continued

Crystallographic parameters for various ternary pnictides, oxides, sulphides and halides.

Compound	Symmetry	Space Group	a/pm	b/pm	c/pm	β/°	Ref.
$(Ca,Ln)_3F_7$ (Ln=Y,La-Lu)*	cubic		552.9				59
Ca_2LnF_7 (Ln=Y,Er-Lu)*	tetragonal		871.1		1666.1		59
Ba_2LnF_8 (Ln=Y,Dy-Lu)*	monoclinic	C2/m	697.8	1051.0	426.0	99.68	60
Ba_2LnF_8 (Ln=Yb,Lu)*	orthorhombic	Pmmn	2190.8	812.0	692.8		60
6H-$RbMgCl_3$	hexagonal		709.5		1757.8		61
4H-$RbMgCl_3$	hexagonal		710		1184		61
9R-$RbMgCl_3$	hexagonal		710		2685		61

* The parameters quoted refer to the element listed first.

powder diffraction studies have shown that quenched samples have a cubic anion excess fluorite structure. Annealing at 773K, however, resulted in (for Ln=Y,Er-Lu) tetragonal superstructure phases, Ca_2LnF_7. Typical unit cell parameters (for $(Ca,Y)_3F_7$ and Ca_2YF_7)[59] are quoted in Table 6 together with similar data for the room temperature monoclinic structures of $BaLn_2F_8$ (Ln=Y, Dy-Lu)[60] and the high temperature orthorhombic structures of $BaLn_2F_8$ (Ln=Yb,Lu).[60]

McPherson, Atwood et al[61] have undertaken a detailed investigation of the structural chemistry of $RbMgCl_3$. Schematic diagrams of the various lattice types exhibited by AMX_3 ternary halides are shown in Figure 2a. Of these, the perovskite, 3C, and the $CsNiCl_3$ type, 2H, are structural extremes; the perovskite consists of octahedra joined at corners while $CsNiCl_3$ consists of octahedra joined only at faces. The other lattice types contain both corner- and face-shared octahedra. Pure $RbMgCl_3$ crystallises in a hexagonal lattice, 6H (Figure 2a), in which there are two crystallographically distinct Mg^{2+} ions. The coordination spheres of one Mg(1) cation and two Mg(2) cations are shown in Figure 2b. The six chloride ions surrounding Mg(1) are equivalent and form a regular octahedron r(Mg(1)...Cl) = 249.4 pm. This octahedron joins corners with six octahedra containing Mg(2) cations. Each of the Mg(2) octahedra also shares a face with a second Mg(2) octahedron; the Mg(2) coordination sphere thus contains two distinct groups of chloride ions with r(Mg(2)...Cl)= 247.0, 250.7 pm. In contrast to the environment of Mg(1), the coordination sphere of Mg(2) is noticeably distorted from that of a regular octahedron. When a small concentration of Ni^{2+} (0.4 - 0.8 mol%) is introduced, $RbMgCl_3$ crystallises in a different hexagonal lattice, 4H (Figure 2a). This structure contains only one type of Mg^{2+} cation; it is similar to the Mg(2) ion of the 6H-structure. At higher Ni^{2+} concentrations ($\sim$4 mol%), a third hexagonal lattice, 9R, (Figure 2a) results. This structure contains two distinct types of Mg octahedra; one is similar to the Mg(2) octahedron of the 6H structure, the other, designated Mg(3), shares two trans-positioned faces with adjacent Mg(2) octahedra. Unit cell parameters for the three structural modifications of $RbMgCl_3$[61] are included in Table 6. The epr spectra of $RbMgCl_3$ crystals doped with Mn^{2+} ions indicate that substitution for Mg^{2+} readily occurs in all three structural

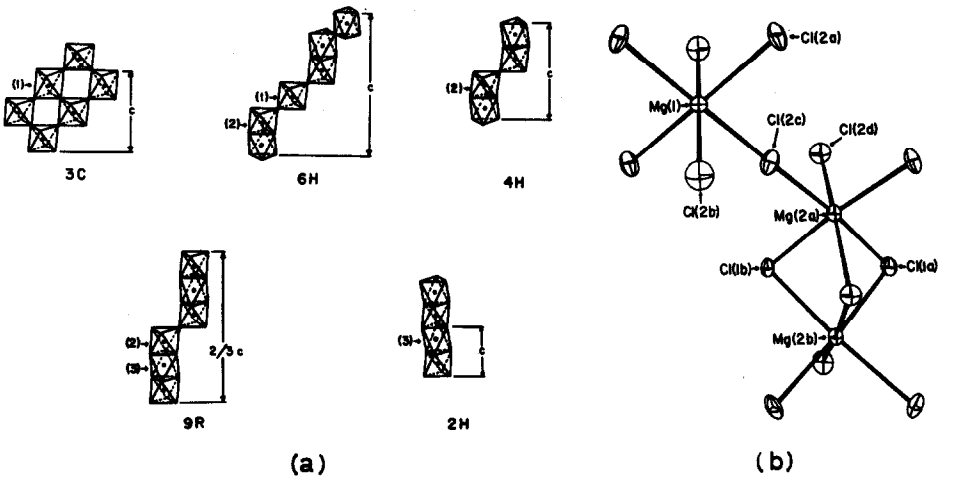

Figure 2. Structural chemistry of $RbMgCl_3$: (a) schematic diagrams of the lattice types for AMX_3 salts (M^{2+} ions lie at the centre and X^- ions lie at the corners of the octahedra); (b) ortep drawing of the coordination spheres of Mg(1) and Mg(2) ions in 6H-$RbMgCl_3$ (reproduced by permission from Inorg. Chem., 20(1981)140).

phases.[61] The magnetic properties of $RbCaF_3$ have also been studied using multinuclear (^{19}F- and ^{87}Rb-) n.m.r. techniques.[62]

2.3.5 Quaternary Derivatives

Once again, Kemmler-Sack[63-78] has written an amazing number (16) of papers on quaternary oxides with variants of the perovskite structure. A major proportion describe the synthesis and characterisation (principally structural and spectroscopic) of hexagonal stacking polytypes with rhombohedral structures; the materials studied, their structural characteristics and unit cell parameters are summarised in Table 7. The structures of the 3L and 6L stacking polytypes are shown in Figure 3; those of the 9L, 12L and 24L variants are shown in earlier reviews.[79,80] The remainder of the papers deal with compounds which adopt distorted perovskite structures and which crystallise in different symmetry classes (cubic, tetragonal, orthorhombic and monoclinic); these compounds are listed in Table 8 together with pertinent unit cell parameters. Kemmler-Sack has also shown that the

Table 7. Crystallographic data for a number of hexagonal stacking polytypes with rhombohedral layer structures.

Compound	Symmetry	Space Group	Stacking Polytype	Layer Sequence	a/pm	c/pm	Ref
$Ba_3[MgM_2O_9]$ (M=Nb,Ta)	hexagonal		3L	$(c)_3$	578	708	63
$Ba_3[CaM_2O_9]$ (M=Nb,Ta)	hexagonal		3L	$(c)_3$	578	707	63
$Ba_5[BaNb_3\boxdot O_{13.5}\boxdot_{1.5}]$	hexagonal	$P6_3/mmc$	5L	(hhccc)	603	1240	63
$Ba_3[InRu_2O_9]$	hexagonal	$P6_3/mmc$	6L	$(hcc)_2$	583	1430	64
$Ba_2[InRuO_6]$	hexagonal	$P\bar{3}m1$	6L	$(hcc)_2$	586	1440	64
$Ba_2[InIrO_6]$	hexagonal	$P\bar{3}m1$	6L	$(hcc)_2$	587	1462	65
$Ba_3[SmIrRuO_9]$	hexagonal	$P6_3/mmc$	6L	$(hcc)_2$	592	1460	65
$Ba_3[SmRu_2O_9]$	hexagonal	$P6_3/mmc$	6L	$(hcc)_2$	592	1470	65
$Ba_3[LnPtRuO_9]$ (Ln=Y,Gd-Lu)	hexagonal	$P6_3/mmc$	6L	$(hcc)_2$	588	1470	66
$Ba_3[LnRu_2O_9]$ (Ln=La,Nd,Sm-Gd,Dy-Yb,Y)	hexagonal		6L	$(hcc)_2$	595	1500	67
$Ba_3[SrM_2O_9]$ (M=Nb,Ta)	hexagonal	$P6_3/mmc$	6L	$(hcc)_2$	606	1530	63
$Ba_2[LaOsO_6]$	rhombohedral	$R\bar{3}m$	6L		607	1478	68
$Ba_3[W_{4/3}Nb_{2/3}\boxdot O_{26/3}\boxdot_{1/3}]$	rhombohedral	$R\bar{3}m$	9L	$(hhc)_3$	584	2090	69
$Ba_3[Nb_2\boxdot O_8\boxdot]$	rhombohedral	$R\bar{3}m$	9L	$(hhc)_3$	604	2120	69
$Ba_2[RhRuO_6]$	rhombohedral	$R\bar{3}m$	9L	$(hhc)_3$	574	2170	64
$Ba_3[RhRu_2O_9]$	rhombohedral	$R\bar{3}m$	9L	$(hhc)_3$	574	2170	64
$Sr_4[M_2Re_2\boxdot O_{12}]$ (M=Co,Ni)	rhombohedral	$R\bar{3}m$	12L	$(hhcc)_3$	554	2670	70
$Ba_4[M_2Re_2\boxdot O_{12}]$ (M=Co,Ni)	rhombohedral	$R\bar{3}m$	12L	$(hhcc)_3$	570	2760	70
$Ba_{7/2}La_{1/2}[MRe_{3/2}W_{1/2}\boxdot O_{12}]$ (M=Co,Ni)	rhombohedral	$R\bar{3}m$	12L	$(hhcc)_3$	569	2760	70

Table 7 continued

Crystallographic data for a number of hexagonal stacking polytypes with rhombohedral layer structures.

Compound	Symmetry	Space Group	Stacking Polytype	Layer Sequence	a/pm	c/pm	Ref
$Ba_4[Ca_{1/2}M_{1/2}Re_2\boxdot O_{12}]$ (M=Co,Ni)	rhombohedral	$R\bar{3}m$	12L	$(hhcc)_3$	576	2780	70
$Ba_4[ScReW\boxdot O_{12}]$	rhombohedral	$R\bar{3}m$	12L	$(hhcc)_3$	575	2780	71
$Ba_4[Re_{9/8}Ta_{13/8}\boxdot_{5/4}O_{12}]$	rhombohedral	$R\bar{3}m$	12L	$(hhcc)_3$	578	2800	72
$Ba_8[Re_{7/2}M_{3/2}\boxdot_3O_{24}]$ (M=Nb,Ta)	rhombohedral	$R\bar{3}m$	24L		582	5550	72
$Ba_{12}[Ba_{8/3}M_{22/3}\boxdot_2O_{33}\boxdot_3]$ (M=Nb,Ta)	rhombohedral	$R\bar{3}m$	36L		592	9300	73

12L-$Ba_2La_{2-x}Ln_x[MgW_2\boxdot O_{12}]$ (Ln=Pr,Sm,Eu,Tb-Tm) and the 18L-$Ba_6[Y_{2-x}Ln_xW_3\boxdot O_{18}]$ (Ln=Sm,Eu,Dy-Er) stacking polytypes, together with the polymorphic perovskites, $Sr_8[SrGd_{2-x}Ln_xW_4\boxdot O_{24}]$ (Ln=Sm,Eu,Dy-Er), exhibit visible photoluminescence.[78]

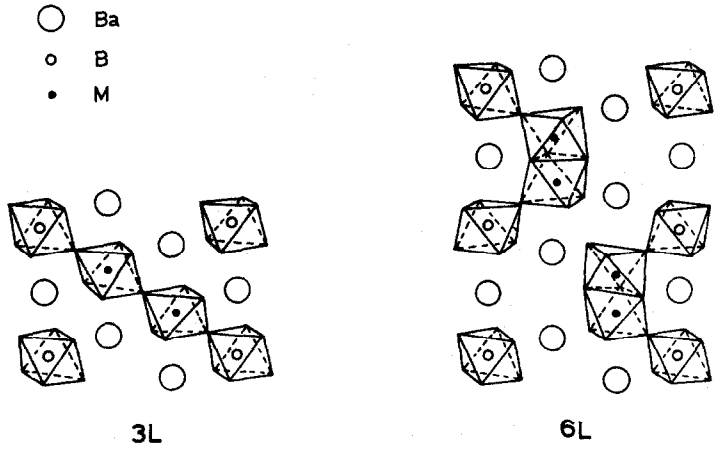

Figure 3. Hexagonal stacking polytypes with rhombohedral layer structures (reproduced by permission from Z. Anorg. Allg. Chem., 479(1981)177).

Several other authors have made contributions to the chemistry of quaternary oxides; without exception they have covered facets of the structural chemistry of these materials. Unit cell parameters for zirconalite, $CaZr_xTi_{3-x}O_7$ ($0.85 \leqslant x \leqslant 1.30$),[81] $SrNdMO_4$ (M=Cr,Mn),[82] $BaSr_2Ln_6O_{12}$ (Ln=Y,Er,Tm),[83] $Ba_4Al_2Ti_{10}O_{27}$,[84] $Ba_6CoNb_9O_{30}$[85] and $BaLn_2Ti_4O_{12}$ (Ln=La-Gd),[86] determined in X-ray diffraction studies, are collected in Table 9. Aspects of the structural chemistry of $BaLn_2Ti_4O_{12}$ (Ln=La-Gd), $BaLn_2Ti_3O_{10}$ (Ln=La-Eu) and $BaLa_2Ti_2O_8$ have also been elucidated from i.r. and Raman spectroscopic data.[87] The structural changes accompanying the ferroelectric phase transitions in $Sr_2(Ta_{1-x}Nb_x)_2O_7$ (x = 0, 0.12) have been studied using temperature dependent single crystal X-ray diffraction methods.[88] Above the Curie points (166K for x = 0, 675K for x = 0.12) the space group of the orthorhombic structure is Cmcm. At lower temperatures, the structures lose the mirror planes at z = 0.25 and z = 0.75 and the metal atoms move along the c axis onto mirror planes at z = 0 and z = 0.5;

Table 8. Unit cell parameters for a number of quaternary oxides with distorted perovskite structures

Compound	Symmetry	a/pm	b/pm	c/pm	β/°	Ref.
$Sr_2[LnSbO_6]$ (Ln=Nd,Sm,Eu,Dy)	monoclinic	587	545	835	90.3	74
$Sr_2[LnSbO_6]$ (Ln=Yb,Lu,Y,Sc)	orthorhombic	579	579	819		74
$Sr_2[LnSbO_6]$ (Ln=Ga,In)	cubic	789				74
$Sr_2[Sr_{1/4}Ln_{1/2}\square_{1/4}WO_6]$ (Ln=La-Nd)	hexagonal	1644		1632		75
$Sr_2[Sr_{1/4}Ln_{1/2}\square_{1/4}WO_6]$ (Ln=Sm,Eu,Gd)HT	cubic	1646				75
$Sr_2[Sr_{1/4}Ln_{1/2}\square_{1/4}WO_6]$ (Ln=Sm,Eu,Gd)LT	hexagonal	995		1900		75
$Sr_2[Sr_{1/4}Ln_{1/2}\square_{1/4}WO_6]$ (Ln=Ho-Lu,Y)	cubic	823				75
$Ba_2[LnSbO_6]$ (Ln=La,Pr,Nd)	monoclinic	668	611	863	90.4	74
$Ba_2[LnSbO_6]$ (Ln=Sm,Eu,Tb,Dy)	cubic	425				74
$Ba_2[LnSbO_6]$ (Ln=Gd,Yb,Lu)	cubic	847				74
$Ba_2[LnOsO_6]$ (Ln=Pr,Nd,Sm-Lu,Y)	cubic	850				68
$Ba_2[Ba_{7/8}\square_{1/8}UO_{47/8}\square_{1/8}]$	tetragonal	1262		1753		76
$Ba_3[BaTa_2O_9]$	orthorhombic	607	1050	1610		63
$Ba_3[EuPtRuO_9]$	monoclinic	591	1024	1480	90.4	66
$Ba_5[BaRe_{3/2}M_{3/2}\square O_{15}]$ (M=Nb,Ta)	orthorhombic	598	1230	607		72
$Ba_5[BaRe_{3/2}Sb_{3/2}\square O_{15}]$	orthorhombic	601	1040	1240		77
$Ba_5[BaW_{3/2}Sb_{3/2}\square O_{27/2}\square_{3/2}]$	orthorhombic	603	1040	1240		77

The crystallographic data refer to the element listed first.

Table 9. Unit cell parameters for a number of diverse quaternary oxides.

Compound	Symmetry	Space Group	a/pm	b/pm	c/pm	β/°	Ref.
$CaZr_xTi_{3-x}O_7$ (x=0.85)	monoclinic	C2/c	1244.4	726.6	1134.1	100.6	81
$SrNdMO_4$ (M=Cr,Mn)*	tetragonal	I4/mmm	384.2		1233.8		82
$BaSr_2Ln_6O_{12}$ (Ln=Y,Er,Tm)*	hexagonal	$P6_3/m$	1029.9		340.9		83
$Ba_4Al_2Ti_{10}O_{27}$	monoclinic	C2/m	1973.7	1134.9	983.7	109.4	84
$Ba_6CoNb_9O_{30}$	tetragonal	P4bm	1258.9		400.9		85
$BaLn_2Ti_4O_{12}$ (Ln=La-Gd)†	orthorhombic	Pba2	2230	1233	386		86

* The crystallographic data refer to the element listed first.

† The crystallographic data refer to $BaPr_2Ti_4O_{12}$

thus although the orthorhombic symmetry is retained the space group changes to $Cmc2_1$.[88]

2.4 COMPOUNDS OF THE ALKALINE EARTH METALS CONTAINING ORGANIC MOLECULES OR COMPLEX IONS

In general, the recently reported chemistry of these compounds is considered in subsections devoted to individual alkaline earth metals; data pertinent to several elements are discussed once only in the subsection of the lightest metal considered. To accommodate the increasing awareness and interest in the role of the alkaline earth metals in bioinorganic chemistry, however, subsections covering salts of carboxylic acids and derivatives of nucleotides and related moieties, have been included.

2.4.1 Salts of Carboxylic Acids

The geometry of calcium-carboxylate interactions in crystalline complexes has been reviewed.[89] They fall into three main categories: a unidentate mode (1) in which the Ca cation binds to only one of the carboxylate oxygen atoms, a bidentate mode (2) in which the carboxylate ion uses both oxygen atoms to chelate the Ca cation and an additional bidentate chelation mode, the α-mode (3) that is observed when a suitable ligating atom for the Ca cation is attached at the α-position and in which chelation of the Ca cation is achieved by the α-substituent together with one of the carboxylate oxygen atoms.[89]

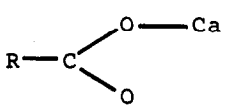

(1)

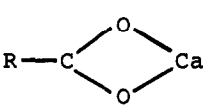

(2)

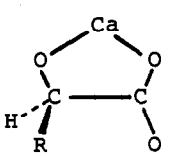

(3)

The molecular structures of calcium oxalate monohydrate (whewellite)[90] and of calcium 2-ethoxybenzoate monohydrate[91] have been elucidated from single crystal X-ray diffraction data. The Ca^{2+} ions eight coordinate in both salts. That in the oxalate is surrounded by seven monodentate oxalate groups, r(Ca...O) = 242.5-246.9 pm and one water molecule, r(Ca...O) = 243.5; that in the

2-ethoxybenzoate is surrounded by two monodentate, r(Ca...O) = 231, 234 pm, and two bidentate, r(Ca...O) = 240-287 pm, carboxylato groups, one ether moiety, r(Ca...O) = 246 pm and one water molecule, r(Ca...O) = 238 pm. Although the Ca^{2+} coordination polyhedron is described as a distorted bicapped trigonal prism for the 2-ethoxybenzoate,[91] no description is proposed for the oxalate.[90]

Alkaline earth metal cations (Mg-Ba) readily form 1:1 complexes with N-(2-hydroxyethyl)ethylenediamine-N,N',N'-triacetic acid.[92] Whereas the dianion is formed for Mg^{2+} and Ba^{2+}, the monoanion is formed for Ca^{2+} and Sr^{2+}. Stability constants and free energies of complexation have been evaluated; the order of the stabilities is

$$Ca^{2+} > Sr^{2+} > Mg^{2+} > Ba^{2+}$$

The solution conformation of the complex formed between Ca^{2+} and ionomycin (a carboxylic acid ionophore) in $CDCl_3$ has been studied by ^{1}H-n.m.r. spectroscopic techniques.[93] It is almost identical to that observed in the crystal;[94] only minor conformational differences in the structure of the ionophore were observed. The significance of these results in the field of cationic transport is discussed.[93]

2.4.2 Complexes of Significance in Bioinorganic Chemistry

The majority of the papers abstracted for this subsection of the review, report on some aspect of solution interaction between alkaline earth metals and biologically significant molecules; ligands studied are many and diverse, varying from nucleotides such as ionosine and cytidine to tetracyclin antibiotics.

Complexation of alkaline earth metal cations (Mg,Ca,Ba) by ionosine and its monoanion has been investigated in aqueous solution at 298K.[95] Comparison of stability constant data with those for 1- and 7-methylinosines and those for guanosine indicates that the preferential binding site of inosine is the N(7) atom of the guanine ring; that of the anion, however, is the N(1) atom of the other ring.[95] Equilibrium constants for the complexation of Mg^{2+} and Ca^{2+} with cytidine[96] and with thiaminemonophosphate and thiaminediphosphate[97] have been determined potentiometrically at 318K. Derived thermodynamic

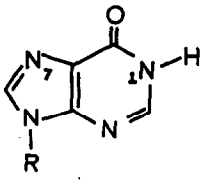

inosine

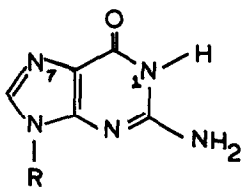

guanosine

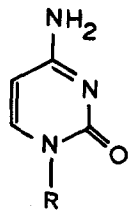

cytidine

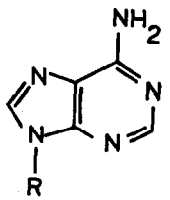

adenosine

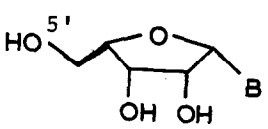

ribose

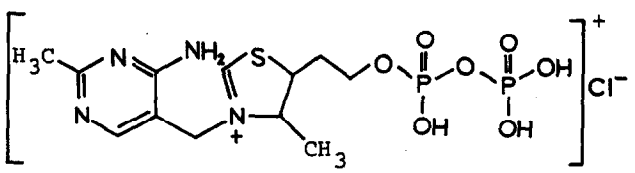

thiamine chloride diphosphate

R = ribose; B = base

data indicate that the formation of the complexes with the thiamine derivatives is favoured by a large positive entropy contribution.[97]

Interactions between Mg^{2+} and guanosine-5'-monophosphate-$[5'\text{-GMP}]^{2-}$,[98] guanosine-5'-triphosphate$[5'\text{-GTP}]^{4-}$,[99] inosine-5'-triphosphate$[5'\text{-ITP}]^{4-}$ [99] and adenosine-5'-triphosphate -$[5'\text{-ATP}]^{4-}$ [99] have been investigated using sophisticated physicochemical methods. The effect of Mg^{2+} on the conformation of $[5'\text{-GMP}]^{2-}$ has been assessed. Evidence that the N(7) atom of the guanine ring is the preferential binding site of guanosine (as for inosine) for Mg^{2+} ions is also reported.[98] The self association tendency of $[5'\text{-ATP}]^{4-}$, $[5'\text{-ITP}]^{4-}$ and $[5'\text{-GTP}]^{4-}$ is promoted by a factor of 3-5 by Mg^{2+} coordination;[99] the effect,

which is attributed to a partial neutralisation effect at the phosphate side chain, is much smaller than that caused by either Zn^{2+} or Cd^{2+} ions. Conformational changes of the -SH group environment in sarcoplasmic reticulum Ca^{2+}-ATPase, induced by the synergistic action of Ca^{2+} and $[5'\text{-ATP}]^{4-}$ have also been studied by e.s.r. methods.[100]

Electronic absorption, circular dichroism and ^{1}H-n.m.r. spectroscopic studies[101] of chlorophylls a and a' and of their Mg^{2+}-free derivatives, pheophytins a and a' and pheophorbides a and a', indicate that the Mg^{2+} ion confers rigidity on the macrocycle. The difference in the spectra of the two groups of compounds are interpreted as arising from both configurational and conformational alterations.[101]

Calorimetric studies[102] of the interaction of Ca^{2+} ions with various methylglycofuranosides (4) in aqueous solutions strongly suggest the formation of 1:1 complexes; the stabilities of these complexes is markedly greater than those of the corresponding Na^{+} ion derivatives.[102] Ultrasonic absorption and ^{13}C chemical shift data[103] both provide evidence for weak complex formation

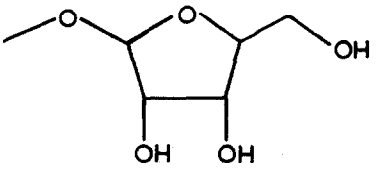

(4)

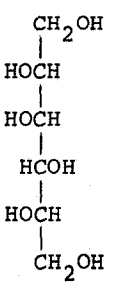

(5)

between Ca^{2+} and D-sorbitol (D-glucitol) (5) in aqueous solution. Although definitive structural data cannot be derived, the ^{13}C-n.m.r. results indicate that the solution structure of the Ca^{2+}-D-sorbitol complex is different from those of the Ln^{3+}-D-sorbital complexes which bond at the hydroxyl groups of the C(2), C(3) and C(4) atoms of the hexose residue.[103]

Complex formation between Ca^{2+} and the tetracyclines, tetracycline(6), oxytetracycline, doxycycline and minocycline has been studied[104] potentiometrically at 310K in aqueous NaCl solution (0.15 mol dm^{-3}). The significance of the results to

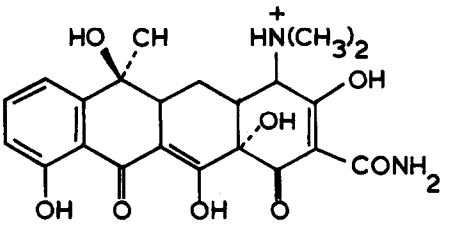

(6)

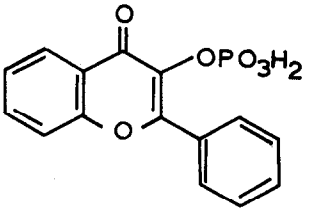

(7)

the mode of action and the distribution of these antibiotics in the human body is discussed.

The binding of Ca^{2+} to humic acids has been studied ($3.9 \leqslant pH \leqslant 5.0$ $275 \leqslant T/K \leqslant 307$)[105] using a radiotracer (^{45}Ca)/ solvent extraction technique; the resultant thermodynamic parameters indicate that a large positive entropy change accounts for the favourable free energy of complexation.

The only complex to be studied by single crystal X-ray diffraction methods is the penta-aquo magnesium salt of flavone-3-monophosphate (7).[106] The molecular structure of the complex consists of hydrophobic layers, which contain the aromatic portions of the flavone residue, and hydrophilic layers which contain the Mg^{2+} ion, the phosphate group and ketonic oxygen of the flavone molecule and the water molecules. The Mg^{2+} ion is octahedrally coordinated by six oxygen atoms derived from four water molecules, r(Mg...O) = 205.8-209.8 pm, the ketonic function, r(Mg...O) = 206.8 pm and the phosphate residue, r(Mg...O) = 203.1 pm, of different anions. Coordination of the Mg^{2+} ion by the ketonic oxygen and the phosphate oxygens results in a seven-membered cis-coordinated chelate ring, $\overline{MgOCCOPO}$.[106]

2.4.3 Beryllium Derivatives

Theoretical (ab initio) calculations have been undertaken for a number of relatively small, beryllium-containing molecules.[107-111] Von Schleyer et al[107] have shown that of the various structural possibilities for $LiBeX_3$ (X=H,F) monomers, there is a distinct preference for attachment of lithium at the edges of BeX_3 triangles (8) rather than to corners or to faces. Von Schleyer et al[107] and Charkin et al[108] have reported complementary results for the minimum energy structure of the Li_2BeX_4 (X=H,F) molecule.

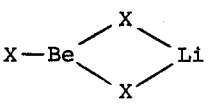

(8)

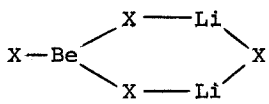

(9)

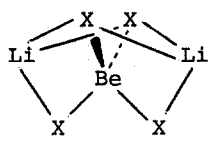

(10)

Although Charkin et al[108] reported without qualification that the planar six-membered cyclic structure (9) is the most favourable configuration for $LiBeH_4$, von Schleyer et al[107] noted that optimum geometries were dependent on the level of the ab-initio MO theory; at the highest level employed Li_2BeH_4 prefers lithium attachment to two faces of a BeH_4 tetrahedron (10); at lower levels, the planar structure (9) is prefered for both Li_2BeH_4 and Li_2BeF_4 (this molecule cannot be studied at the higher level).

Marynik[109] has calculated the relative stabilities of $R^tBeR^b_2BeR^t$ dimers and the corresponding monomers, R^tBeR^b (R^t = H, CH_3,F,BH_4,C_5H_5,C_6H_5; R^b = H,CH_3,C_6H_5). The effect of substituents in the R^t position has been assessed; whereas C_5H_5 groups strongly disfavour dimerisation, and CH_3 or F substituents slightly destabilise the dimers, BH_4 substituents provide a small dimer stabilisation. Furthermore, phenyl bridging is shown to be highly favoured vis-a-vis methyl bridging.[109]

Glidewell et al have reported the results of theoretical calculations on BeR_2 and BeHR (R = Me,CH=CH_2,C≡CH,CN and C_5H_5),[110] $CH_{4-n}(BeH)_n$ and $[CH_{4-n}(BeH)_n]^+$ ($0 \leqslant n \leqslant 4$),[110] and the beryllium derivatives of $(CH)_n$ ($3 \leqslant n \leqslant 8$) carbocycles.[111] Optimum geometries calculated for BeR_2 and BeHR have symmetries in precise agreement with the predictions of the Jahn Teller theorem.[110] For the $CH_{4-n}(BeH)_n$ and $[CH_{4-n}(BeH)_n]^+$ series, the calculated barriers to inversion via a planar intermediate are lower for the cations than for the molecular species and decrease with increasing n until they are zero for $[CH(BeH)_3]^+$ and $[C(BeH)_4]^+$. Indeed the minimum energy of these two cations occurs when strictly planar at the carbon atom.[110] Optimum geometry calculations for the beryllium derivatives of $(CH)_n$ ($3 \leqslant n \leqslant 8$) moieties, give stable minima for C_4H_4 at $(h^4\text{-}C_4H_4)Be$ of C_{4v} symmetry, $(h^4\text{-}C_4H_4)_2Be$ (D_{2h}) and $(h^2\text{-}C_4H_4)_2Be$ (C_{2h}), for C_6H_6 at $(h^2\text{-}C_6H_6)Be$ (C_{2v}), $(h^2\text{-}C_6H_6)_2Be$ (D_{2d}), $(h^1\text{-}C_6H_6)(h^2\text{-}C_6H_6)Be$ (C_s) and $(h^2,h^2\text{-}C_6H_6)Be_2$ (C_s), for C_7H_7 at $(h^3\text{-}C_7H_7)BeH$ (C_s) and for C_8H_8 at $(h^2\text{-}C_8H_8)Be$ (C_s) and $(h^2,h^2\text{-}C_8H_8)Be_2$ (C_{2h}). C_3H_3 does

not give any h^3-derivatives, the beryllium atom always undergoing insertion into the ring to form a beryllaheterocycle.[111]

Spectrophotometric studies[112] of the reaction of Be^{2+} with a number of monoazo-derivatives of pyrocatechol (11) have been

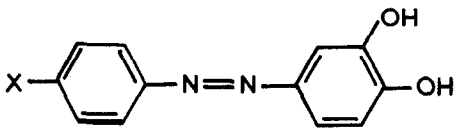

X=H; CH_3; Cl; SO_3H; NO_2.

(11)

effected. A complex with a 1:1 Be:ligand ratio is formed; it is thought to contain a Be_2O^{2+} cation coordinated by two ligand molecules through the functional dihydroxyl grouping.[112]

Partition coefficients of the complexes formed between Be^{2+} and the β-diketonates, acetylacetone, propionylacetone, 3-methylacetylacetone and 3-ethylacetylacetone have been determined[113] in aqueous $NaClO_4$/n-hexane systems as a function of temperature ($278 \leqslant T/K \leqslant 318$) and of $NaClO_4$ concentration ($0 \leqslant c/mol\ dm^{-3} \leqslant 3$). The results are interpreted in terms of water structure changes (i.e., hydrophobic hydration) amd of specific hydration in the outer coordination sphere of the coordinatively saturated chelates (i.e., hydration of the bonded ligands).[113]

Solvent extraction of alkaline earth metal ions in aqueous $NaClO_4$ or NaSCN ($1 mol\ dm^{-3}$)/hexane systems using trioctylphosphine oxide (topo) has been studied at 298K.[114] The extraction in both systems improved in the sequence:

$$Be^{2+} > Ca^{2+} > Sr^{2+} \sim Mg^{2+} \sim Ba^{2+}$$

The poor extraction of Mg^{2+} salts was attributed to their strong hydration. For equivalent topo concentrations, Be^{2+} and Ca^{2+} were extracted more effectively as the perchlorate and Ba^{2+} was extracted more effectively as the thiocyanate; the choice of anion was immaterial for Mg^{2+} and Sr^{2+}. These results are thought to show that (i) $M(ClO_4)_2$ (M=Be-Ba) and $M(SCN)_2$ (M=Sr,Ba) are extracted as ion pairs, $[M(topo)_4]^{2+}(X^-)_2$ ($X=ClO_4$ or SCN), (ii) $Be(SCN)_2$ is extracted as solvates of neutral species, $Be(SCN)_2(topo)_n$ (n=2,3), and (iii) $M(SCN)_2$ (M=Mg,Ca) should

exhibit both ionic and coordinative properties in the organic phase.[114]

Metallation of borato(phosphoniomethanide)(phosphoniooxide) (12) with tertiary butyl lithium at 195K in thf/pentane leads to a lithium complex (13) which reacts in situ with $BeCl_2$ to form the spirocyclic beryllium complex (14);[115] this latter complex has been characterised by i.r., multinuclear (^1H- and ^{13}C-) n.m.r. and mass spectroscopic methods.

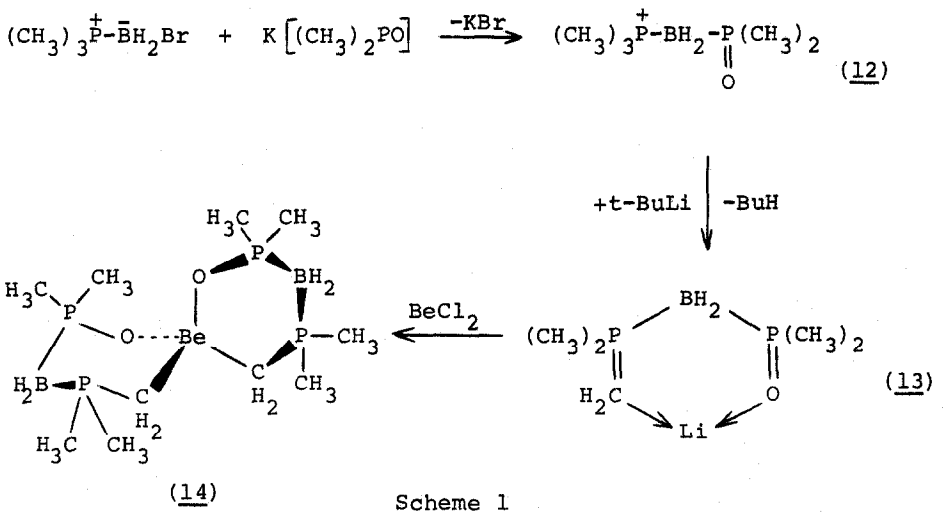

Scheme 1

Reaction of $(h^5\text{-}C_5H_5)BeCl$ with $K[B_5H_8]$ in a pentane slurry at 233K has afforded $[\mu\text{-}(h^5\text{-}C_5H_5)Be][B_5H_8]$.[116] A low temperature (173K) single crystal X-ray diffraction study has shown that the structure of this product is similar to that of $[B_5H_9]$ with a hydrogen bridge replaced by a bridging $(h^5\text{-}C_5H_5)Be$ moiety, r(Be...B) = 204.5, 205.5 pm. The beryllium atom is centred above the cyclopentadienyl ring with r(Be...C) = 187.7-189.4 pm.[116]

The molecular structure of the diethyl ether solvate of disodium di-μ-hydrido-bis(diethylberyllate) has also been ascertained.[117] It is composed of $[Be_2Et(\mu\text{-}H)_2]$ anions with pairs of Na^+ cations, each coordinated to one disordered solvate molecule, r(Na...O) = 235.0 pm, lying about alternate centres of symmetry along a (Figure 4). The anions are isoelectronic with $[B_2Et_4(\mu\text{-}H)_2]$ and contain Be-H-Be three centre two electron pair bonds, r(Be...H) = 144, 153 pm, which are analogous to those in

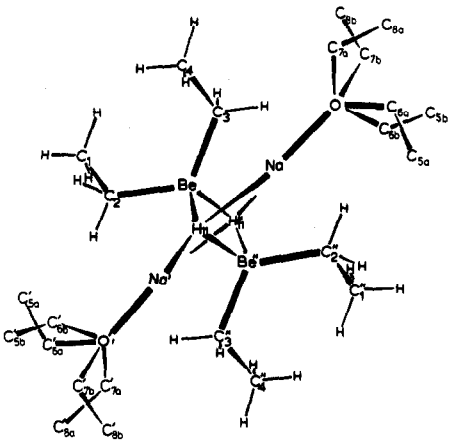

Figure 4. Perspective view of the molecular structure of $Na_2[Be_2Et_4(\mu\text{-}H)_2].2H_2O$ (reproduced by permission from Acta Crystallogr., B37(1981)68).

in boron hydrides. The pseudo tetrahedral coordination polyhedron of the Be atom is completed by two carbon atoms of the ethyl residues, r(Be...C) = 176.6, 181.0 pm. The similarity in the environment of the bridging hydrogen atoms vis-a-vis beryllium and sodium (Figure 4) suggests that the Na...H and Be...H interactions may be similar in character.[117]

2.4.4 Magnesium Derivatives

Although there are a vast number of publications dealing with magnesium chemistry, but few are abstracted for this review; the majority of published papers are ignored as they are associated with organomagnesium chemistry, a subject reviewed in detail elsewhere.[2,3]

A recurrent feature of the structural chemistry of inorganic magnesium derivatives is the $[Mg(H_2O)_6]^{2+}$ cation; it occurs in the structures of both $[Mg(H_2O)_6]_2[CdCl_6]$[118] and the 2:1 molecular complex of caffeine with $[Mg(H_2O)_6]Br_2$.[119] The former complex consists of two crystallographically distinct $[Mg(H_2O)_6]^{2+}$ octahedra, r(Mg(1)...O) = 204.1, 209.6 pm, r(Mg(2)...O) = 207.1 pm joined by hydrogen bonds and $[CdCl_6]^{2-}$ octahedra.[118] The latter complex contains $[Mg(H_2O)_6]^{2+}$ octahedra, r(Mg...O) = 206.6-208.4pm, uncoordinated caffeine molecules and bromide anions held together

by a network of hydrogen bonds.[119]

Dissociation enthalpies for $[Mg(H_2O)_n]Cl_2$ (n=4,6) have been calculated[120] from dissociation pressure data for these materials; they are collected in Table 10.

Complexation of Mg^{2+} by 3-hydroxy-2-methyl-1,4-naphthoquinone monoxime[121] and of Mg^{2+} and Ca^{2+} by ethylenediamine tetra-acetic acid[122] has been studied by potentiometric[121] and n.m.r.[122] methods. The n.m.r. results suggest that a pH-dependent equilibrium is set up between the uncomplexed cation and the edta-metal cation complex. The kinetics of ligand exchange on $[Mg(OPPh_3)_5]^{2+}$ has been studied by ^{31}P n.m.r. techniques;[123] the process is thought to proceed via a dissociative mechanism, the rate being independent of free ligand. The results are compared with corresponding data for exchange on $[Zn(OPPh_3)_4]^{2+}$.[123]

Cyclopentadienyl magnesium hydride, has been prepared conveniently by reaction of MgH_2 with cyclopentadiene in thf.[124] It is readily soluble in thf and is thought to adopt a dimeric structure with bridging hydrogen atoms (15); the pseudo-tetrahedral coordination of the Mg atom is completed by the cyclopentadienyl ring and a thf solvate molecule. Its reactions with selected aromatic ketones, trityl halides and polynuclear hydrocarbons are described.[124]

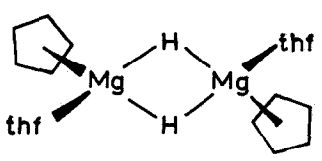

(15)

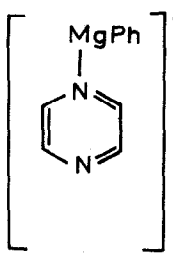

(16)

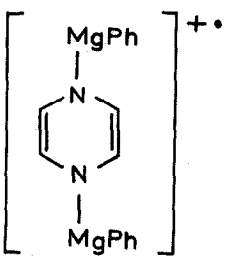

(17)

A reinvestigation of the reduction of pyridine by MgH_2, effected by de Konig et al,[125] has proven unambiguously that the final product is the bis(pyridine) complex of bis(1,4-dihydro-1-pyridyl) magnesium. The claim of Ashby and Goel[126] that the product of this reaction also contains 1,2-dihydro-1-pyridyl moieties after extended reaction periods has been traced, by de Konig et al, to the presence of aluminium bound hydrogen in the MgH_2 used by Ashby and Goel.

Treatment of pyrazine with diphenyl magnesium in thf leads, via an electron transfer reaction, to the 1:1 radical complex (16).[127]

Table 10. Dissociation enthalpies for $[Mg(H_2O)_n]Cl_2$ (n=4,6) and for $[Ca(NH_3)_n]Cl_2$ (n=1,2,4,8).[120]

n	ΔH_{diss} (1/n$[Mg(H_2O)_n]Cl_2$,c,298K) kJ.mol^{-1}	n	ΔH_{diss} (1/n$[Ca(NH_3)_n]Cl_2$,c,298K) kJ.mol^{-1}
4 (second law)	66.3±1.2	1	78.2±0.8
4 (third law)	67.0±0.4	2	67.8±0.8
6 (second law)	58.3±0.2	4	42.0±0.3
6 (third law)	58.6±0.1	8	44.4±0.3

In the presence of sodium or potassium a persistent 1:2 radical complex (17) is formed. Although diphenyl beryllium does not undergo the former reaction, a beryllium analogue of the 1:2 radical complex (17) has been formed under similar conditions. The complexes were characterised by e.s.r. spectroscopy.[127]

Ashby and Goel[128-130] have continued their studies of the chemistry of magnesium methylcuprates. Mixtures of "CH_3MgBr" and CuBr in thf (the so-called Normant reagent) have been found to contain, depending on the time and temperature of the reaction, the following magnesium methylcuprates: $MgCu(CH_3)_2$, $Mg_2Cu_3(CH_3)_7$, $MgCu_2(CH_3)_4$, $MgCu_3(CH_3)_5$, $MgCu_4(CH_3)_6$ and $MgCu_6(CH_3)_8$.[128] Characterisation of complexes was established by complete elemental analysis of both solution phase and solid products at selected temperatures and after certain reaction times. Their identity was confirmed in a comparative study of the n.m.r. spectra of the solutions with those of authentic samples prepared independently by reactions of CuBr or MeCu with Me_2Mg in appropriate stoichiometric ratios as shown in scheme 2.[128]

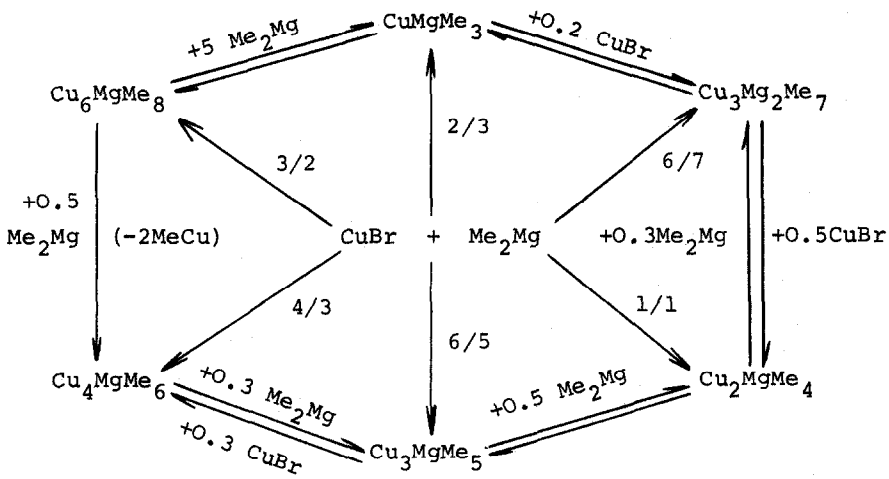

Scheme 2

The species in the Normant reagent responsible for addition to phenylacetylene (which was used as a model system) were found to be $MgCu_4(CH_3)_6$ and $MgCu_6(CH_3)_8$.[129] The magnesium methylcuprates, $MgCu(CH_3)_3$ and $MgCu_2(CH_3)_4$ have also been identified as products of the reactions of $[(COD)CuBr]_2$ with Me_2Mg and "RMgBr".[130]

$MgCu(CH_3)_3$, a previously unknown complex, is stable in thf for over 48 hours at ambient temperature (298K) and for at least 168 hours at 273K.

Structural analyses have been performed on $[LiMg(CH_3)_3tmen]$,[131] $[MgTiCl_6(CH_3COOC_2H_5)_4]$[132] and $[Mg(C{\equiv}CPh)_2(tmen)_2]$.[133] Reaction of $(CH_3Li)_4$ with $(CH_3)_2Mg$ in dry ether containing tmen gave both $[LiMg(CH_3)_3tmen]$ and $[Li_2Mg(CH_3)_4(tmen)_2]$.[131] The structure of the former complex was elucidated from single crystal X-ray diffraction data and that of the latter inferred by comparison; details are given in Section 1.5.8. Single crystals of $[MgTiCl_6(CH_3COOC_2H_5)_4]$ were obtained by reaction of $MgCl_2$ with $TiCl_4$ in dry $CH_3COOC_2H_5$.[132] X-ray diffraction studies showed that the complex has a chlorine bridged structure (18) in which both metal atoms are octahedrally coordinated. The Ti atom is

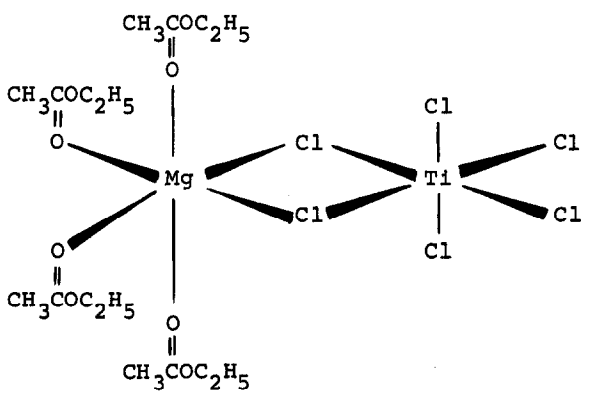

(18)

surrounded by six chlorine atoms, $r(Ti...Cl_t)$ = 229.3, $r(Ti...Cl_b)$ = 248.0 pm and the Mg atom is surrounded by the two bridging chlorine atoms, $r(Ti...Cl_b)$ = 252.8 pm and the carbonyl oxygen atoms of the four ester molecules, r(Mg...O) = 203.8 pm.[132] $[Mg(C{\equiv}CPh)_2(tmen)_2]$ has been prepared from $Mg(C{\equiv}CPh)_2$ and tmen in toluene and investigated by X-ray diffraction methods.[133] The structure is shown in Figure 5; it is said to represent the first example of an organomagnesium compound with octahedral coordination of the Mg atom. The phenylethynyl ligands are in trans positions, r(Mg...C) = 217.6, 220.0 pm, as are the bidentate tmen ligands, r(Mg...N) = 237.5 pm.

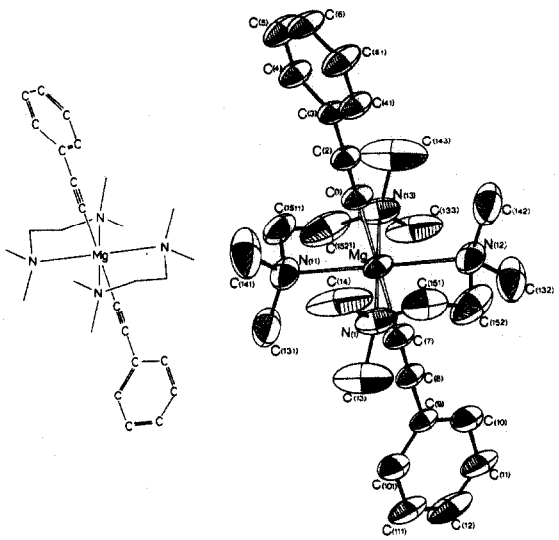

Figure 5. Schematic representation and ortep diagram of the molecular structure of $[Mg(C{\equiv}CPh)_2(tmen)_2]$ (reproduced by permission from Chem. Ber. 114(1981)2640).

2.4.5 Calcium, Strontium and Barium Derivatives

The application of ^{43}Ca-n.m.r. techniques to an elucidation of the immediate chemical environment of Ca^{2+} ions in aqueous and non-aqueous solutions has been attempted.[134] Unfortunately, the low natural abundance of the ^{43}Ca isotope (0.13%) and the low sensitivity of the nucleus ($I=^{7}/2$; sensitivity = 6.4×10^{-2} c.f. ^{1}H at constant field) renders it difficult to work with these solutions. Nevertheless, it has been shown that the ^{43}Ca resonance in these solutions is quite sensitive to the immediate chemical environment of the Ca^{2+} ions.[134]

Interaction between $CaCl_2$ and formamide leads to three complex compounds, $CaCl_2,(HCONH_2)_n$ (n=2,4,6);[135] they have all been characterised by chemical, X-ray diffraction, i.r., ^{1}H-n.m.r. and dta-tga analyses.

Distorted pentagonal bipyramidal Ca^{2+} coordination polyhedra are observed in the structures of calcium methanedisulphonate trihydrate[136] and tris(glycine) calcium diiodide monohydrate.[137] That in the methanedisulphonate consists of seven oxygen atoms, three from water molecules, r(Ca...O) = 224.2-240.0 pm and four

from one bidentate and two monodentate anions. The ligand forms a six-membered ring with one Ca^{2+} ion, r(Ca...O) = 237.0, 244.6pm, and is linked to two other Ca^{2+} ions by unidentate bonds, r(Ca...O) = 234.9, 241.3 pm.[136] That in the tris(glycine) complex consists of seven oxygen atoms, two from water molecules, r(Ca...O) = 241, 257 pm, and five from monodentate glycine molecules, r(Ca...O) = 228-250 pm.[137]

The structures of $[Ca(NH_3)_8]Cl_2$ and of $[Ca(NH_3)_2]Cl_2$ have been derived from X-ray powder diffraction data (obtained using a Guinier-Hogg camera and a computer based film scanner system) and refined using the Rietveld full-profile technique.[138] Whereas the Ca^{2+} environment in the octa-ammine is a distorted triangular prism of NH_3 molecules, r(Ca...N) = 252-272 pm, in the diammine it is an irregular octahedron of two NH_3 molecules, r(Ca...N) = 237, 274 pm and four Cl^- anions, r(Ca...Cl) = 274-282 pm.[138] Dissociation enthalpies for $[Ca(NH_3)_n]Cl_2$ (n=1,2,4,8) have been calculated from dissociation pressure data for these materials;[120] they are collected in Table 10.

Solutions of hexaphenylethane (hpe) in aromatic solvents, (benzene, toluene) react with strontium and barium mirrors forming deep red-brown solutions of bis(triphenylmethyl)strontium and bis(triphenylmethyl)barium.[139] The products can be isolated as stable solid compounds by removal of solvent under vacuum. Although reaction with barium occurs at room temperature (298K), significant reaction does not start with strontium until 333K; with calcium no reaction was observed even at 373K.[139]

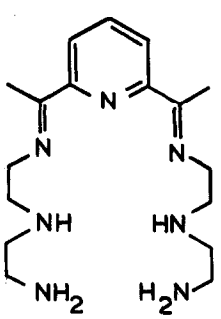

(19)

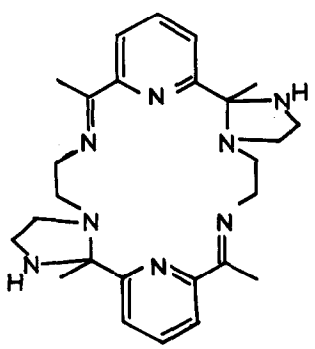

(20)

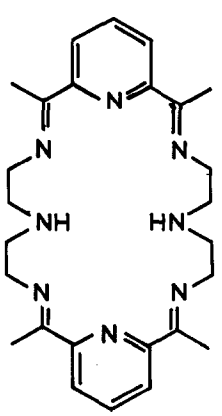

(21)

Reaction of 2,6-diacetylpyridine with diethylenetriamine in the presence of alkaline earth metal (Mg-Ba) salts in methanol at room temperature yields complexes of the open-chain Schiff-base ligand (19).[140] The use of higher reaction temperatures affords complexes (Mg^{2+} excepted) of the macrocyclic ligand (20). The intermediacy of the (19) complexes in the (20) macrocycle formation has been proven by their subsequent ring closure reactions both in the presence and absence of added diketone. Single crystal X-ray diffraction studies have been effected on $[(20).Ba(ClO_4)_2]$.[140] The Ba^{2+} ion is ten-coordinate being bonded to the six nitrogen atoms of the macrocyclic ring in an approximately planar array, r(Ba...N) = 284.1-289.1 pm, and to four oxygen atoms of two perchlorate anions in pseudo axial positions, r(Ba...O) = 292.3-306.0 pm. The single coordinated alkaline earth metal ion in the (20) complexes may be replaced by two Cu^{2+} or two Ag^{+} ions with accompanying expansion of the macrocycle to the 24 membered (tetraimine) form (21). The reversibility of the (20)⇌(21) expansion/contraction has been established.[140]

REFERENCES

1 P.Hubberstey, Coord. Chem. Rev., 40(1982)64.
2 A.Maercker, J. Organomet. Chem., 211(1981)1.
3 J.Villieras, J. Organomet. Chem., 223(1981)1.
4 J.Evers, G.Oehlinger, A.Weiss, C.Probst, M.Schmidt and P.Schramel, J. Less Common Metals, 81(1981)15.
5 Y.Hasegawa, H.Wakabayashi, M.Sakuma and T.Sekine, Bull. Chem. Soc. Japan, 54(1981)2427.
6 K.G.Heumann and H.-P.Schiefer, Z. Naturforsch., 36b(1981)566.
7 K.G.Heumann and H.Kloppel, Z. Anorg. Allg. Chem., 472(1981)83.
8 P.Hubberstey, Coord. Chem. Rev., 34(1981)51.
9 S.Tamaki, Y.Tsuchiya and Y.Waseda, J. Phys. F: Metal Phys., 11(1981)1865.
10 A.Palenzona, J. Less Common Metals, 78(1981)P49.
11 A.Widera and H.Schäfer, J. Less Common Metals, 77(1981)29.
12 D.Marshall and Y.A.Chang, J. Less Common Metals, 78(1981)139.
13 G.Bruzzone, E.Franceschi and F.Merlo, J. Less Common Metals, 81(1981)155.
14 M.L.Fornasini,F.Merlo and K.Schubert, J. Less Common Metals, 79(1981)111.
15 F.Merlo and M.L.Fornasini,Acta Crystallogr., B37(1981)500.
16 W.B.Pearson, Acta Crystallogr., B37(1981)1174.
17 W.B.Pearson, Acta Crystallogr., B37(1981)1183.
18 W.B.Pearson, J. Less Common Metals, 80(1981)59.
19 H.Leuken, J. Less Common Metals, 79(1981)151.
20 E.Veleckis, J. Less Common Metals, 80(1981)241.
21 M.Notin and J.Hertz, J. Less Common Metals, 80(1981)P1.
22 C.B.Magee, J. Liu and C.E.Lundin, J. Less Common Metals, 78(1981)119.
23 T.Hirata, T.Matsumoto, M.Amano and Y.Sasaki, J. Phys. F: Metal Phys., 11(1981)521.
24 K.Ensslen, H.Oesterreicher and E.Bucher, J. Less Common Metals, 77(1981)287.
25 Z.Gavra, Z.Hadari and M.H.Mintz, J. Inorg. Nucl. Chem., 43(1981)1763.
26 H.Imamura and S.Tsuchiya, J. Chem. Soc. Chem. Commun., (1981)567.
27 P.S.Bakhshi, V.K.Jain and J.Shanker, J. Inorg. Nucl. Chem., 43(1981)901.
28 E.Brechtel, G.Cordier and H.Schäfer, Z. Naturforsch., 36b(1981)1341.
29 F.Hulliger and T.Siegrist, Z. Naturforsch., 36b(1981)14.
30 H.P.Beck, Z. Naturforsch., 36b(1981)1255.
31 R.Thomas and F.H.Moore, Acta Crystallogr., B37(1981)2153.
32 R.Thomas and F.H.Moore, Acta Crystallogr., B37(1981)2156.
33 A.A.Luginina, L.A.Ol'khovaya, D.D.Ikrami, V.M.Reiterov and A.S.Paramzin, Russ. J. Inorg. Chem., 26(1981)178.
34 E.G.Prout, E.G.Shephard and C.T.O'Connor, J. Inorg. Nucl. Chem., 43(1981)643.
35 E.G.Prout and E.G.Shepard, J. Inorg. Nucl. Chem., 43(1981)1977.
36 H.Einaga, J. Inorg. Nucl. Chem., 43(1981)229.
37 K.Matsumoto and T.Sata, Bull. Chem. Soc. Japan, 54(1981)674.
38 I.J.F.Poplett and J.A.S.Smith, J. Chem.Soc. Faraday Trans. II, 77(1981)235.
39 E.Brechtel, G.Cordier and H.Schäfer, Z. Naturforsch., 36b(1981)1099.
40 E.Brechtel, G.Cordier and H.Schäfer, J. Less Common Metals, 79(1981)131.

41 G.Pouillard, M.Shamsulalam, M.-C.Trinel-Dufour and P.Perrot, J. Chem. Research, (S), (1981)136.
42 A.A.Fotiev and V.V.Strelkov, Russ. J. Inorg. Chem., 25(1980)1569.
43 A.A.Fotiev and V.V.Strelkov, Russ. J. Inorg. Chem., 25(1980)1292.
44 G.LeFlem, P.Courbin, C.Delmas and J.-L.Soubeyroux, Z. Anorg. Allg. Chem., 476(1981)69.
45 D.Chales de Beaulieu and H.Muller-Buschbaum, Z. Anorg. Allg. Chem., 472(1981)33.
46 V.K.Trunov, I.M.Averina and Y.A.Velikodnyi, Sov. Phys. Crystallogr., 26(1981)222.
47 K.Sander and H.Muller-Buschbaum, Z. Anorg. Allg. Chem., 478(1981)52.
48 M.Schweizer and H.Muller-Buschbaum, Z. Anorg. Allg. Chem., 482(1981)173.
49 V.D.Zhuravlev and A.A.Fotiev, Russ. J. Inorg. Chem., 25(1980)1414.
50 N.-H.Chan, R.K.Sharma and D.M.Smyth, J. Electrochem. Soc., 128(1981)1762.
51 V.L.Volkov, Russ. J. Inorg. Chem., 25(1980)1299.
52 V.N.Tsygankov, N.V.Porotnikov, K.I.Petrov and E.S.Nosova, Russ. J. Inorg. Chem., 26(1981)1215.
53 G.Blasse and P.H.M.De Korte, J. Inorg. Nucl. Chem., 43(1981)1505.
54 I.S.Shaplygin and V.B.Lazarev, Russ. J. Inorg. Chem., 26(1981)24.
55 M.Ghedira, J.Chenavas, F.Sayetat, M.Marezio, O.Massenet and J.Mercier, Acta Crystallogr., B37(1981)1491.
56 H.D.Rad and R.Hoppe, Z. Anorg. Allg. Chem., 483(1981)7.
57 H.D.Rad and R.Hoppe, Z. Anorg. Allg. Chem., 483(1981)18.
58 P.P.Fedorov and L.A.Ol'khovaya, Russ. J. Inorg. Chem., 26(1981)115.
59 O.Greis and M.Kieser,Z. Anorg. Allg. Chem., 479(1981)165.
60 O.Greis, P.Stede and M.Kieser, Z. Anorg. Allg. Chem., 477(1981)133.
61 K.O.Devaney, M.R.Freedman, G.L.McPherson and J.L.Atwood, Inorg. Chem., 20(1981)140.
62 E.A.Vopilov, V.N.Voronov, V.A.Vopilov and V.M.Buznik, J. Struct. Chem., 22(1981)131.
63 S.Kemmler-Sack, I.Thumm and M.Herrmann, Z. Anorg. Allg. Chem., 479(1981)177.
64 H.-U.Schaller and S.Kemmler-Sack, Z. Anorg. Allg. Chem., 473(1981)178.
65 I.Thumm, U.Treiber and S.Kemmler-Sack, Z. Anorg. Allg. Chem., 477(1981)161.
66 S.Kemmler-Sack, A.Ehmann and M.Herrmann, Z. Anorg. Allg. Chem., 479(1981)171.
67 U.Treiber, S.Kemmler-Sack, A.Ehmann, H.-U.Schaller, E.Durrschmidt, I.Thumm and H.Bader, Z. Anorg. Allg. Chem., 481(1981)143.
68 U.Treiber and S.Kemmler-Sack, Z. Anorg. Allg. Chem., 478(1981)223.
69 S.Kemmler-Sack and U.Treiber, Z. Anorg. Allg. Chem., 478(1981) 198.
70 M.Herrmann,S.Kemmler-Sack, Z. Anorg. Allg. Chem., 476(1981) 115.
71 S.Kemmler-Sack and M.Herrmann, Z. Anorg. Allg. Chem., 480(1981)171.

72 S.Kemmler-Sack and A.Ehmann, Z. Anorg. Allg. Chem., 483(1981)165.
73 S.Kemmler-Sack., Z. Anorg. Allg. Chem., 476(1981)109.
74 U.Wittmann, G.Rauser and S.Kemmler-Sack., Z. Anorg. Allg. Chem., 482(1981)143.
75 S.Kemmler-Sack and A.Ehmann, Z. Anorg. Allg. Chem., 479(1981)184.
76 U.Treiber, A.J.Griffiths and S.Kemmler-Sack, Z. Anorg. Allg. Chem., 473(1981)171.
77 S.Kemmler-Sack and A.Ehmann, Z. Anorg. Allg. Chem., 483(1981)161.
78 S.Kemmler-Sack, Z. Anorg. Allg. Chem., 483(1981)126.
79 P.Hubberstey, Coord. Chem. Rev., 40(1982)77.
80 P.Hubberstey, Coord. Chem. Rev., 34(1981)58.
81 B.M.Gatehouse, I.E.Grey, R.J.Hill and H.J.Rossell, Acta Crystallogr., B37(1981)306.
82 K.Sander, U.Lehmann and H.Muller-Buschbaum, Z. Anorg. Allg. Chem., 480(1981)153.
83 A.-R.Schulze and H.Muller-Buschbaum, Z. Naturforsch., 36B(1981)837.
84 J.Schmachtel and H.Muller-Buschbaum, Z. Anorg. Allg. Chem., 472(1981)89.
85 U.Lehmann and H.Muller-Buschbaum, Z. Anorg. Allg. Chem., 481(1981)7.
86 A.M.Gens, M.B.Varfolomeev, V.S.Kostomarov and S.S.Koronin, Russ. J. Inorg. Chem., 26(1981)482.
87 N.V.Porotnikov, K.I.Petrov, A.M.Gens and M.B.Varfolomeev, Russ. J. Inorg. Chem., 25(1980)1606.
88 N.Ishizawa, F.Marumo and S.Iwai, Acta Crystallogr., B37(1981)26.
89 H.Einspahr and C.E.Bugg, Acta Crystallogr., B37(1981)1044.
90 S.Deganello, Acta Crystallogr., B37(1981)826.
91 N.J.Ray and B.J.Hathaway, Acta Crystallogr., B37(1981)1652.
92 R.P.Mathur and P.N.Mathur, Indian. J. Chem., 20A(1981)309.
93 M.J.O.Anteunis and G.Verhegge, Bull. Soc. Chim. Belg., 90(1981)1153.
94 P.Hubberstey, Coord. Chem. Rev., 34(1981)68.
95 H.Lonnberg and P.Vihanto, Inorg. Chim. Acta., 56(1981)157.
96 B.T.Khan and R.M.Raju, Indian. J. Chem., 20A(1981)860.
97 B.T.Khan, P.N.Rao and M.M.Khan, Indian. J. Chem., 20A(1981)857.
98 T.Theophanides and M.Polissiou, Inorg. Chim. Acta, 56(1981)L1.
99 K.H.Scheller, F.Hofstetter, P.R.Mitchell, B.Prijs and H.Sigel, J. Am. Chem. Soc., 103(1981)247.
100 P.Laggner, J.Suko, C.Punzengruber and R.Prager, Z. Naturforsch., 36b(1981)1136.
101 P.H.Hynninen and G.Sievers, Z. Naturforsch., 36b(1981)1000.
102 A.Vesala and H.Lonnberg, Acta Chem. Scand., A35(1981)123.
103 J.K.Beattie and M.T.Kelso, Austral. J. Chem., 34(1981)2563.
104 M.Brion, G.Berthan and J.-B.Furtillan, Inorg. Chim. Acta, 55(1981)47.
105 G.R.Choppin and P.M.Shanbhag, J. Inorg. Nucl. Chem., 43(1981)921.
106 R.Bergstrom, K.Satyshur and M.Sundaralingam, Acta Crystallogr., B37(1981)254.
107 E.-U.Wurthwein, M.-B.Krogh-Jespersen and P. von R.Schleyer, Inorg. Chem., 20(1981)3663.
108 A.I.Boldyrev, L.P.Sukhanov, V.G.Zakzhevskii and O.P.Charkin, Russ. J. Inorg. Chem., 26(1981)306.

109 D.S.Marynick, J. Am. Chem. Soc., 103(1981)1328.
110 C.Glidewell, J. Organomet. Chem., 217(1981)273.
111 J.R.Bews and C.Glidewell, J. Organomet. Chem., 219(1981)279.
112 N.N.Basargin, Y.G.Rozovskii, L.D.Sokolova and L.M.Kurbanova, Russ. J. Inorg. Chem., 26(1981)1101.
113 J.Narbutt, J. Inorg. Nucl. Chem., 43(1981)3343.
114 S.Kusakabe and T.Sekine, Bull. Chem. Soc. Japan, 54(1981) 2930.
115 H.Schnidbaur and E.Weiss, Angew. Chem. Int. Ed. Engl., 20(1981)283.
116 D.F.Gaines, K.M.Coleson and J.C.Calabrese, Inorg. Chem., 20(1981)2185.
117 G.W.Adamson, N.A.Bell and H.M.M.Shearer, Acta Crystallogr., B37(1981)68.
118 M.Ledesert and J.C.Monier, Acta Crystallogr., B37(1981)652.
119 M.Biagini-Cingi, A.M.Manotti-Lanfredi, A.Tiripicchio, G.Bandoli and D.A.Clemente, Inorg. Chim. Acta, 52(1981)237.
120 R.W.Carling, J. Chem. Thermodyn., 13(1981)503.
121 A.Kamini, S.K.Sindhwani and R.P.Singh, Indian J. Chem., 20A(1981)1040.
122 E.Bouhoutsos-Brown, D.Murk Rose and R.G.Bryant, J. Inorg. Nuclear Chem., 43(1981)2247.
123 S.F.Lincoln, D.L.Pisaniello, T.M.Spotswood and M.N.Tkaczuk, Austral. J. Chem., 34(1981)283.
124 A.B.Goel and E.C.Ashby, J. Organomet. Chem., 214(1981)C1.
125 A.J. de Koning, P.H.M.Budzelaar, B.G.K. van Aarssen, J.Boersma and G.J.M. van der Kerk, J. Organomet. Chem., 217(1981)C1.
126 E.C.Ashby and A.B.Goel, J. Organomet. Chem., 204(1981)139.
127 W.Kaim, Z. Naturforsch., 36b(1981)1110.
128 E.C.Ashby, A.B.Goel and R.Scott-Smith, J. Organomet. Chem., 212(1981)C47.
129 E.C.Ashby, R.Scott-Smith and A.B.Goel, J. Organomet. Chem., 215(1981)C1.
130 A.B.Goel and E.C.Ashby, Inorg. Chim. Acta, 54(1981)L199.
131 T.Greiser, J.Kopf, D.Thoennes and E.Weiss, Chem. Ber., 114(1981)209.
132 J.C.J.Bart, I.W.Bassi, M.Calcaterra, E.Albizzati, U.Giannini and S.Parodi, Z. Anorg. Allg. Chem., 482(1981)121.
133 B.Schubert, U.Behrens and E.Weiss, Chem. Ber., 114(1981)2640.
134 R.M.Farmer and A.I.Popov, Inorg. Nucl. Chem. Letters, 17(1981)51.
135 M.N.Nabiev, M.R.Yugai, S.Tukhtaev, O.F.Khodzhaev, B.M.Beglov and I.K.Irgashev, Russ. J. Inorg. Chem., 26(1981)811.
136 A.Karipides, Acta Crystallogr., B37(1981)2232.
137 S.Natarajam and J.K.Mohana Rao, J. Inorg. Nucl. Chem., 43(1981)1693.
138 S.Westman, P.-E.Werner, T.Schuler and W.Raldow, Acta Chem. Scand., A35(1981)467.
139 B.I.Nakhmanovich, E.V.Kristal'nyi, R.V.Basova, Z.H.Baidakova and A.A.Arest-Yakubovich, Doklady Chem., 255(1980)520.
140 M.G.B.Drew, J.Nelson and S.M.Nelson, J. Chem. Soc. Dalton Trans., (1981)1678.